SLAC-PUB-13587
April 2009

MEASUREMENTS, ANALYSIS, AND SIMULATION OF MICROWAVE INSTABILITY IN THE LOW ENERGY RING OF KEKB*

Yunhai Cai
SLAC National Accelerator Laboratory
Stanford University
Menlo Park, CA 94025, USA

J. Flanagan, H. Fukuma, Y. Funakoshi,
T. Ieiri, K. Ohmi, K. Oide, and Y. Suetsugu
KEK, Oho, Tsukuba, Ibaraki 305-0801, Japan

Abstract

Using a streak camera, we measured the longitudinal profiles of a positron bunch in the Low Energy Ring (LER) of KEKB at various currents. The measured charge densities were used to construct a simple Q=1 broadband impedance model. The model, with three parameters, not only gave an excellent description of longitudinal dynamics for positive momentum compaction factor but also for the negative ones, including bunch shortening below a threshold and bursting modes above the threshold. Furthermore, our study indicated that the threshold of microwave instability was about 0.5 mA in bunch current in the LER. At the nominal operating current 1.0 mA, there was a 20% increase of the energy spread. The results of measurement, analysis, and simulations will be presented in this paper.

Presented at Particle Accelerator Conference, Vancouver, Canada, May 4-8, 2009

*Work supported by the Department of Energy under Contract No. DE-AC02-76SF00515.

MEASUREMENTS, ANALYSIS, AND SIMULATION OF MICROWAVE INSTABILITY IN THE LOW ENERGY RING OF KEKB*

Yunhai Cai, SLAC National Accelerator Laboratory, Menlo Park, CA 94025, USA
J. Flanagan, H. Fukuma, Y. Funakoshi, T. Ieiri, K. Ohmi, K. Oide, Y. Suetsugu,
KEK, Oho, Tsukuba, Ibaraki 305-0801, Japan

Abstract

Using a streak camera, we measured the longitudinal profiles of a positron bunch in the Low Energy Ring (LER) of KEKB at various currents. The measured charge densities were used to construct a simple Q=1 broadband impedance model. The model, with three parameters, not only gave an excellent description of longitudinal dynamics for positive momentum compaction factor but also for the negative ones, including bunch shortening below a threshold and bursting modes above the threshold. Furthermore, our study indicated that the threshold of microwave instability was about 0.5 mA in bunch current in the LER. At the nominal operating current 1.0 mA, there was a 20% increase of the energy spread. The results of measurement, analysis, and simulations will be presented in this paper.

INTRODUCTION

Let's consider an electron in a storage ring executing a small synchrotron oscillation in a stationary RF bucket. For simplicity, we introduce a normalized coordinate system, $q = z/\sigma_z$ and $p = -\delta/\sigma_\delta$, where z is the differential position relative to the synchronized particle with energy E_0, $\delta = (E - E_0)/E_0$, and σ_z and σ_δ are the standard deviations of position and relative energy in the equilibrium Gaussian distribution at zero beam current. Here we use positive q as the forward direction of the beam. It is well known that the bunch length $\sigma_z = \alpha c\sigma_\delta/\omega_s$, where ω_s is the angular frequency of the synchrotron oscillation and α is the momentum compaction factor. The motion of the electron is that of a simple harmonic oscillator described by the Hamiltonian, $H = \frac{1}{2}(q^2 + p^2)$, along with independent variable $\theta = \omega_s t$.

In general, the electron also experiences a collective force induced by the bunch distribution $\lambda(q)$. Using the notion of an integrated wakefield $W(q)$ in a single turn, the dynamics can be described by a Hamiltonian

$$H = \frac{1}{2}(q^2 + p^2) - I_n \int_{-\infty}^{q} dq'' \int_{-\infty}^{\infty} dq' \lambda(q') W(q'' - q'),$$

where

$$I_n = \frac{r_e N_b}{2\pi\nu_s\gamma\sigma_\delta} \tag{1}$$

is the normalized current, which was introduced by Oide and Yokoya [1], N_b represents the number of electrons in the bunch, ν_s is the synchrotron tune, r_e is the classic radius of electron, and $\gamma = E_0/mc^2$. Here, the bunch distribution $\lambda(q)$ has been normalized, namely $\int_{-\infty}^{\infty} \lambda(q)dq = 1$.

It is worth noting that the dynamics effect of the wakefield is scaled by the normalized current I_n. Its dependence on the parameters in Eq. (1) clearly shows that we prefer a higher energy, faster synchrotron oscillation, or larger relative energy spread to reduce the effects of the wakefield. Although, it does not explicitly depend on the momentum compaction factor α, for a negative $\alpha < 0$, one needs to use a negative normalized current as well, namely $I_n < 0$. Moreover, if W(q) is given in terms of V/pC, one should convert I_n from meter to pC/V.

Furthermore, it can be shown that the evolution of beam density distribution $\Psi(q, p)$ is governed by the Vlasov-Fokker-Planck (VFP) equation

$$\frac{\partial\Psi}{\partial\theta} - \{H, \Psi\}_{PB} = 2\beta\frac{\partial}{\partial p}(p\Psi + \frac{\partial\Psi}{\partial p}), \tag{2}$$

where $\beta = 1/\omega_s\tau_d$ and τ_d is the longitudinal damping time. We use the subscript PB to indicate the Poisson Bracket. Actually, H is the Hamiltonian defined previously with the substitution of $\lambda(q) = \int_{-\infty}^{\infty} \Psi(q, p)dp$. As a result, the VFP equation is a nonlinear integral and partial differential equation. In general, it can only be solved by numerical methods [2]. In fact, it is a special form of the Fokker-Planck equation since the damping and diffusion terms on the right-hand side involve only the partial derivatives of p. This is a consequence of the fact that the synchrotron radiation causes loss and quantum diffusion only in the energy of the radiating electron not in its time of flight.

HAISSINSKI SOLUTIONS

Historically, it was Haissinski who discovered that the VFP equation (Eq. 2) has a static solution in the form of [3]

$$\begin{aligned} \Psi_0(q, p) &= \frac{1}{\kappa\sqrt{2\pi}} \exp(-H_0) \\ &= \lambda_0(q) \exp(-\frac{p^2}{2})/\sqrt{2\pi} \end{aligned} \tag{3}$$

Here the subscript "0" indicates that the solution does not explicitly depend on θ or $\partial\Psi/\partial\theta = 0$. Since Ψ_0 is a function of the Hamiltonian H_0 only, it commutes with H_0 in the Poisson Bracket; therefore the right hand side of the equation vanishes by itself.

On the other hand, Ψ_0 is also factorized into a product of a Gaussian distribution in p and $\lambda_0(q)$, which makes the

* Work supported by the Department of Energy under Contract No. DE-AC02-76SF00515.

right hand side of the equation vanish separately. Eliminating the dependence of p in Eq. (3), we find the well-known Haissinski integral equation

$$\lambda_0(q) = \exp[-\frac{q^2}{2} + I_n \int_{-\infty}^{\infty} dq' \lambda_0(q') S(q-q')]/\kappa, \quad (4)$$

where $S(q) = \int_{-\infty}^{q} W(q')dq'$ and κ is a constant determined by the normalization condition, $\int_{-\infty}^{\infty} \lambda_0(q)dq = 1$. At zero current, $I_n = 0$, so the solution becomes a Gaussian. In general, this nonlinear integral equation can be solved numerically using Newton's Iteration starting from the Gaussian distribution. In practice, we know that the Haissinski distribution is not just a possible solution but also the equilibrium distribution of the VFP equation at a sufficiently low current. Above a threshold of I_n, the Haissinski distribution is no longer a stable solution. In the literature, the associated instability is commonly referred to as the microwave instability.

SIMULATION

The VFP equation can be solved [2] using a two-dimensional grid to represent the distribution in phase space. Motivated by the necessity to extend the simulation to six-dimensional phase space in the future, we introduce macro particles to represent the phase-space distribution

$$\Psi(q,p) = \frac{1}{N_p} \sum_{i=1}^{N_p} \delta(q-q_i)\delta(p-p_i), \quad (5)$$

where q_i, p_i are the canonical coordinates of the particles so that the evolution of $\Psi(q,p)$ can be carried out by tracking the particles.

For each step of $\Delta\theta$, we use three integration steps based on the technique of splitting operators. First, we apply a kick generated by the wakefield $W(q)$

$$\Delta p_i = I_n \int_{-\infty}^{\infty} dq' \lambda(q') W(q_i - q')\Delta\theta. \quad (6)$$

To speed up the calculation, we deposit the charge of every particle onto two adjacent grid points with a linear weighting to accumulate $\lambda(q)$ on a one-dimensional mesh. The integration is replaced by a summation over the grid and the kicks on all the grid points are calculated and stored. For the kick on the particle, we use a linear interpolation of kicks on the two adjacent grids. In the second step, we simply have a rotation

$$\begin{aligned} q_i &= \cos(\Delta\theta) q_i + \sin(\Delta\theta) p_i, \\ p_i &= -\sin(\Delta\theta) q_i + \cos(\Delta\theta) p_i, \end{aligned} \quad (7)$$

which is a solution of the free harmonic oscillator. In the final step, we apply the radiation damping and quantum excitation

$$\Delta p_i = -2\beta p_i \Delta\theta + \sqrt{12\beta\Delta\theta}\xi(i), \quad (8)$$

where ξ is a random number generated by a uniform distribution between -1 to 1. As an example shown in Fig. 1, we make a direct comparison between the VFP solver[2] and our PIC simulation. One can see from the figure that there is not much difference and both give a good description of the saw-tooth instability including its periodicity.

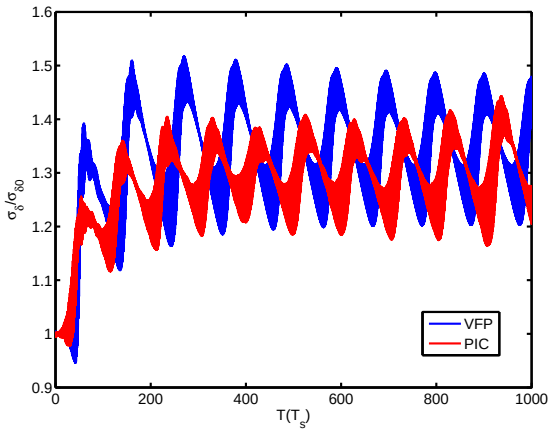

Figure 1: *A comparison between VFP and PIC codes using the impedance of the SLC damping ring [4]. The number of macro particles is chosen to be the same as the number of grid points in the VFP solver.*

IMPEDANCE MODEL

In general, one needs to collect all possible impedance sources, such as bellows, masks, and collimators, and calculate their impedance, and construct a wakefield $W(q)$ by adding up all contributions in the entire storage ring. For simplicity, we choose the Q=1 broadband resonance as our impedance model.

For a parallel LRC circuit, the non-vanishing wakefield, for $q < 0$, is given by

$$W(q) = w_0[\cos(Aq) + \sin(Aq)/\sqrt{4Q^2-1}]\exp(x_r q/2Q),$$

where $A = x_r\sqrt{1-1/4Q^2}$ and $x_r = \omega_r\sigma_z/c$. One can easily convert three dynamical parameters Q, x_r, w_0 to their engineering counterparts L, R, C by using

$$\begin{aligned} L &= w_0(\sigma_z/x_r c)^2, & (9)\\ R &= Q w_0(\sigma_z/x_r c), & (10)\\ C &= 1/w_0. & (11) \end{aligned}$$

It has been known from previous work by Ieiri and Koiso that the LER, like many modern storage rings, was rather inductive. By fitting to a pure inductance impedance model, they found that its inductance $L = 96$ nH. These inductances more or less fix another parameter in the broadband model. However, there is still a tradeoff between x_r and w_0 to be made according to Eq. (9). The necessary information is provided by the measurement of the positron beam profiles using a streak camera. The data is shown in

the top plot of Fig. 2. It is clear that the measured shapes are essentially Gaussians; we have to choose $x_r \geq 2$ to avoid a shoulder in the distributions at high currents. In the bottom plot of Fig. 2, we show the Haissinski distributions times the beam currents at the corresponding currents.

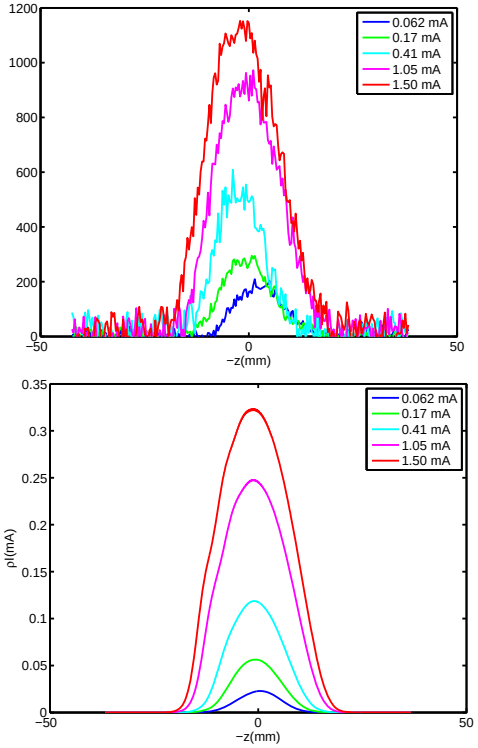

Figure 2: Comparisons of bunch profiles of the measurement using a streak camera and products of the Haissinski distributions and the corresponding beam currents.

The final selection of the parameters x_r and w_0 are actually made using a compromise between the fitting to the measured bunch lengths shown in Fig. 3 and the matching to the beam profiles. We settle on the values of $x_r = 3$ and $w_0 = 5 \times 10^5 m^{-1}$, which correspond to $L = 116$ nH, $R = 22.9$ KΩ, and $C = 0.22$ fF. The results of the fitting to the measurements are shown in the plots of Fig. 3. Note that the PIC simulations are necessary to fit the measured bunch lengths.

For positive α, as one can see in Fig. 3 the simulated distributions start to deviate from the Haissinski distributions beyond the value of 0.5 mA of the bunch current. According to the theory of microwave instability, the threshold is $I_{th} = 0.5$mA. At the operating current of 1.0 mA, we have a 20% increase of energy spread in the simulation.

One pleasant surprise is that the impedance model also gives good agreement with the measurement when α switches to its negative value as shown in Fig. 3. Incidentally, its threshold of microwave instability is also at 0.5 mA. Slightly above the threshold, at $I_b = 0.6$ mA, we see a bursting mode in the simulation, which was consistent with the observation.

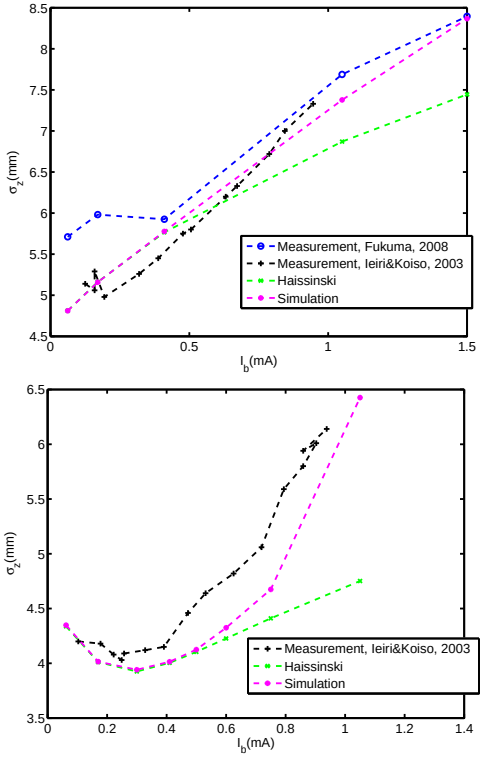

Figure 3: Measurements of bunch length compared to simulations and Haissinski solutions for both positive $\alpha = 3.4 \times 10^{-4}$ (top) and negative $\alpha = -3.4 \times 10^{-4}$ (bottom).

CONCLUSION

Our study of the microwave instability was remarkably successful. We have shown that the simple broadband impedance models enabled us to explain many measurements and observations including the bunch shortening and lengthening, the shapes of beam profiles at various beam currents, and the thresholds of microwave instability and the bursting modes. Most important is the fact that the prediction of the growth of the energy spread was confirmed by a measurement [5] using the particle detector Belle. The success can be attributed to several advances we have made. First, we found that it is critical to use the results of the simulation to fit the measured bunch length because the microwave instability contributes additional lengthening to the Haissinski solutions. Second, we learned that shapes of the distributions are essential to narrow down the type of impedances.

REFERENCES

[1] K. Oide and K. Yokoya, KEK-Preprint-90-10, April (1990).

[2] R. Warnock and J. Ellison, SLAC-PUB-8404, (2000).

[3] J. Haissinski, *Nuovo Cimenta* **18B**, 72 (1973).

[4] K. Bane and C. Ng, SLAC-PUB-6254, April (1993).

[5] Y. Cai *al al.*, SLAC-PUB-13570, April (2009).